

New opportunities for 3D materials science of polycrystalline materials at the micrometre lengthscale by combined use of X-ray diffraction and X-ray imaging

W. Ludwig^{a,b,*}, A. King^{b,c}, P. Reischig^b, M. Herbig^a, E.M. Lauridsen^d, S. Schmidt^d, H. Proudhon^e, S. Forest^e, P. Cloetens^b, S. Rolland du Roscoat^b, J.Y. Buffière^a, T.J. Marrow^c, H.F. Poulsen^d

^a Université de Lyon, INSA-Lyon, MATEIS CNRS UMR 5510, 69621 Villeurbanne, France

^b European Synchrotron Radiation Facility, BP220, 38043 Grenoble, France

^c School of Materials, University of Manchester, Manchester, M13 9PL, UK

^d Risø National Laboratory for Sustainable Energy, Technical University of Denmark, P.O. Box 49, DK-4000 Roskilde, Denmark

^e MINES ParisTech, Centre des matériaux, CNRS UMR 7633, BP 87, 91003 Evry Cedex, France

ARTICLE INFO

Article history:

Received 25 February 2009

Received in revised form 2 April 2009

Accepted 3 April 2009

Keywords:

3D grain mapping

Diffraction contrast tomography

Polycrystals

Holotomography

Topotomography

3DXRD

ABSTRACT

Non-destructive, three-dimensional (3D) characterization of the grain structure in mono-phase polycrystalline materials is an open challenge in material science. Recent advances in synchrotron based X-ray imaging and diffraction techniques offer interesting possibilities for mapping 3D grain shapes and crystallographic orientations for certain categories of polycrystalline materials. Direct visualisation of the three-dimensional grain boundary network or of two-phase (duplex) grain structures by means of absorption and/or phase contrast techniques may be possible, but is restricted to specific material systems. A recent extension of this methodology, termed X-ray diffraction contrast tomography (DCT), combines the principles of X-ray diffraction imaging, three-dimensional X-ray diffraction microscopy (3DXRD) and image reconstruction from projections. DCT provides simultaneous access to 3D grain shape, crystallographic orientation and local attenuation coefficient distribution. The technique applies to the larger range of plastically undeformed, polycrystalline mono-phase materials, provided some conditions on grain size and texture are fulfilled. The straightforward combination with high-resolution microtomography opens interesting new possibilities for the observation of microstructure related damage and deformation mechanisms in these materials.

© 2009 Elsevier B.V. All rights reserved.

1. Introduction

Over the past decade significant progress in three-dimensional, hard X-ray imaging has been achieved by applying the principles of computerized tomography to projection images formed by contrast mechanisms that have become available with the advent of 3rd generation synchrotron sources [1–3]. The aim of this paper is to illustrate some of the possibilities these new imaging techniques provide for the investigation of polycrystalline materials. The examples presented share a common experimental setup for synchrotron radiation X-ray microtomography (SR μ CT) and exploit three different types of contrast: (i) absorption contrast, (ii) phase contrast arising from propagation and interference phenomena under coherent illumination (Fresnel diffraction) and (iii) image contrast arising from Bragg diffraction. In all cases the sample is illuminated by an extended (2D), parallel beam of monochromatic

X-rays and a series of projection images is recorded on a high-resolution 2D detector system while the sample is rotated around a fixed axis.

Among these different contrast mechanisms, X-ray attenuation (typically dominated by X-ray photo absorption) is the simplest to exploit. The intensity distribution measured in the transmitted beam can, in most cases (neglecting redistribution due to scattering), be directly interpreted in terms of mathematical projections of the attenuation coefficient distribution inside the sample. Acquisition of a large number of projections and the use of well established arithmetic reconstruction algorithms gives access to the three-dimensional distribution of the X-ray attenuation coefficient [4]. Quantitative, three-dimensional absorption imaging employing monochromatic radiation is performed at various synchrotron installations worldwide and requires only the selection of an appropriate X-ray energy for the sample dimensions and composition, and a detector system of suitable size and resolution.

The observation of propagation based phase contrast (Fresnel diffraction, inline holography) [5,6] requires in addition to monochromaticity, some degree of spatial coherence of the X-ray beam. Third generation synchrotron sources perfectly meet these

* Corresponding author at: Université de Lyon, INSA-Lyon, MATEIS CNRS UMR 5510, 69621 Villeurbanne, France. Fax: +33 4 76 88 22 52.

E-mail address: ludwig@esrf.fr (W. Ludwig).

requirements and extensive use of this additional contrast mechanism has allowed some of the restrictions commonly encountered in conventional absorption imaging to be overcome (i.e. poor contrast for low Z materials and between materials of similar X-ray attenuation coefficient). For instance, phase contrast can reveal interphase boundaries and small defects (cracks, porosities, inclusions) undetectable in absorption contrast [7]. Some variants of quantitative phase contrast imaging (Bonse Hart interferometry [8], grating interferometry [9], diffraction enhanced imaging [10], holotomography [11]) require the sample to fulfill conditions in terms of absorption, total phase shift or maximum phase gradients.

In general, neither absorption nor phase contrast can reveal the three-dimensional grain structure in polycrystalline materials. There are, however, a few exceptions to this rule. Specific processing routes in certain material systems can lead to the formation of layer like precipitation of a second phase located at the grain boundaries of the matrix material, in which case absorption and/or phase contrast tomography may reveal the three-dimensional shape information (see Section 2). However, no information about the crystallographic grain orientation can be obtained from these images.

The two-dimensional distribution of fine grained crystalline phases can be revealed by means of X-ray diffraction tomography [12,13]. This variant of monochromatic beam X-ray microdiffraction can be readily combined with fluorescence detection and provides insight into the spatial arrangement of crystalline phases and trace elements in heterogeneous multiphase materials. Efforts are underway to extend this kind of scanning approaches and to resolve shape and orientation of individual crystallites in fine grained mono-phase materials. The extension to three-dimensions is done by stacking of slices. However, as for any point scanning approach, time restrictions apply for the characterization of three-dimensional sample volumes.

Three-dimensional mapping of large grained polycrystalline materials in terms of orientation and 3D grain shapes can be achieved by combining the principles of X-ray diffraction imaging (topography) [14] and image reconstruction from projections (computerized tomography). The X-ray diffraction contrast tomography (DCT) [15,16,17] technique presented later in this paper may be regarded as a variant of the previously introduced 3D XRD methodology (see Ref. [18] for a review) and applies to the case of plastically undeformed materials, exhibiting limited values of misorientation spread inside individual grains. This condition ensures that diffraction spots can be treated as parallel projections of the grains. Note that three-dimensional characterization of deformed microstructures is possible, but requires slower and more elaborate data acquisition and analysis procedures, employing above mentioned scanning microbeam diffraction approaches.

A variety of acquisition and reconstruction strategies for analysing image contrast related to Bragg diffraction have been explored so far [21–26]. The focus in this paper will be on two variants, closest to conventional X-ray tomography: X-ray diffraction contrast tomography [15–17] (Section 3) and topotomography [27,28], a variant of the technique that allows imaging of one individual bulk grain with improved spatial and/or temporal resolution (Section 4). An example illustrating the combined use of X-ray diffraction contrast tomography and microtomography is presented in Section 5.

2. 3D imaging of grain structures by X-ray absorption and phase contrast

Due to their sub-nanometre width, the local difference in X-ray attenuation or electron density variation at grain boundaries cannot directly be imaged by parallel beam X-ray absorption and/or phase

contrast imaging techniques. However, for some specific material systems it is possible to reveal the grain structure by decorating the grain boundary network with a thin film of a second phase having different X-ray attenuation and/or electron density.

A first possibility to achieve grain boundary decoration is by penetration and wetting of the grain boundary network by a liquid phase, as observed during the processes of liquid metal embrittlement and grain boundary wetting [29]. One prominent material system, ideally suited for direct inspection by X-ray absorption contrast microtomography is the embrittlement of Aluminium and its alloys by liquid Gallium. The embrittlement process leads to the formation of liquid Ga wetting layers up to several hundred nanometres thick [30,31], visible as bright, highly absorbing lines in the 2D tomographic slice displayed in Fig. 1a. It has to be emphasised that the Ga infiltration technique modifies the mechanical properties of the material and has to be considered as a destructive characterization technique. Nevertheless this imaging modality can be used for post-mortem analysis of crack propagation and crack-grain interactions in Aluminium alloys [32–36].

Another possible mechanism for the decoration of grain boundaries is the preferential precipitation and segregation of alloying elements at grain boundaries that act as nucleation sites for phase transformations in two-phase metallic alloys. The differences in density and composition between phases of different crystal structure may be too weak to be detected in absorption contrast. In these cases different variants of coherent X-ray imaging techniques, providing up to two orders of magnitude gain in sensitivity, may still reveal the presence of sub-micrometre second phase layers delineating the position of grain boundaries. In its simplest variant, propagation based, differential phase contrast imaging can be performed in the so-called edge detection regime, by adjusting the sample to detector distance D to values comparable to $D = 1/2 \lambda f^2$, where λ is the X-ray wavelength and f the spatial frequency of the objects to be detected with optimum contrast [6]. Fig. 2b shows a reconstructed cross section of a metastable beta (bcc) Titanium alloy (TIMET $\beta 21S$) which can be heat treated in such way that layer like precipitation of alpha (hcp) phase occurs at the grain boundaries between beta grains [37]. The different crystal structure and the partitioning of alloying elements between these two phases during annealing creates an electron density difference that can be easily detected at a propagation distance of 150 mm (see Fig. 2b).

The gain in sensitivity provided by use of phase contrast can be assessed from comparison with Fig. 2a showing the same cross section in conventional absorption contrast ($D = 7$ mm).

As a final example we mention the possibility to reveal the spatial distribution of phases in *two-phase* microstructures as encountered for instance in some duplex stainless steel or titanium alloys. Although phase contrast tomography based on a single distance can reveal the position of the interphase boundaries, the segmentation of the two-phase structure by conventional thresholding or region growing algorithms may fail if there is insufficient difference in grayvalues (attenuation coefficient) between the phases. The acquisition of several tomographic scans at different propagation distances allows one performing a two step reconstruction process yielding a quantitative reconstruction of the refractive index decrement δ ($n = 1 - \delta + i\beta$), proportional to the electron density in the material. In this procedure, termed holotomography [11] one first calculates a projection of the phase shift (based on projection images at different distances) and, in a second step, the three-dimensional distribution of the refractive index decrement. Fig. 3 shows a comparison of the different contrast mechanisms (absorption, phase sensitive tomography, holotomography) applied to a two-phase (austenitic, ferritic), stainless steel microstructure in the as cast condition.

Apart the specificity (the above mentioned examples have to be considered as exceptions—for most engineering alloys the grain

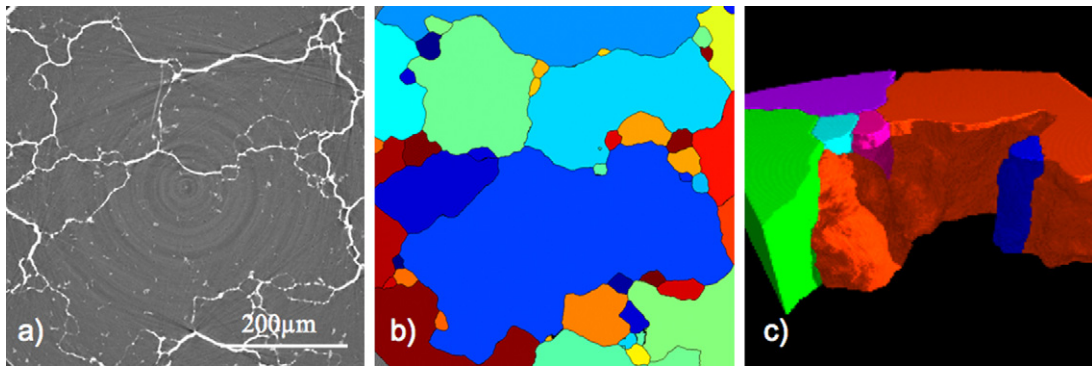


Fig. 1. (a) absorption contrast microtomography of hot extruded sample made from Aluminum alloy AA5083, infiltrated by liquid Gallium. (b) Result of (3D) segmentation procedure based on mathematical morphology. (c) 3D rendition of grain structure.

structure cannot be revealed by either of these variants), the examples shown so far have another common shortcoming: none of them gives access to crystallographic information (orientation, lattice parameters) required for a full description of the grain microstructure. As demonstrated in the next section, these limitations can be overcome for a certain class of materials by combining the principles of X-ray diffraction imaging (topography) [14] and image reconstruction from projections (computerized tomography).

3. 3D mapping of grain structures by X-ray diffraction contrast tomography

X-ray diffraction contrast tomography [15–17] is a variant of the previously introduced 3DXRD technique [18] enabling simultaneous reconstruction of the 3D grain shapes and orientations in

suitable polycrystalline materials. The technique shares a common experimental setup with the conventional SR μ CT introduced in section one. In both cases, the sample is placed on a rotation stage and irradiated by an extended, parallel and monochromatic synchrotron X-ray beam. For the case of polycrystalline materials, each of the grains will pass through Bragg diffraction alignments multiple times during the sample rotation, producing diffracted beams (reflections). Beams diffracted at small angles will be captured on the detector system that covers an area substantially bigger than the sample (Fig. 4). In the absence of orientation and strain gradients inside the grains, the diffracted beams form two-dimensional spots that can be treated as parallel projections of the diffracting grain. The analysis of Friedel pairs of these diffraction spots allows one to determine the crystallographic orientation and 3D shape of the grains in the sample [17]. The processing route can be summarised as follows:

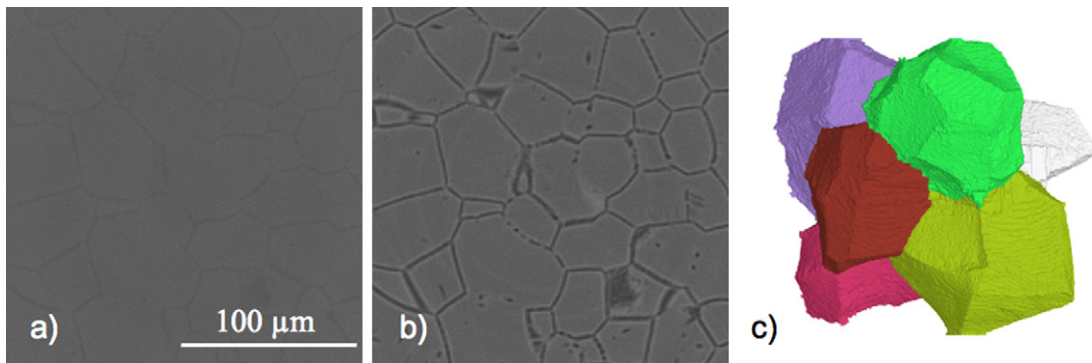


Fig. 2. (a) Tomographic reconstruction of heat treated Ti alloy sample at a propagation distance of $D = 7$ mm (absorption tomography). (b) Identical slice for a scan acquired at a propagation distance of $D = 150$ mm (phase sensitive tomography). (c) 3D rendition of grain cluster as obtained from morphological image segmentation.

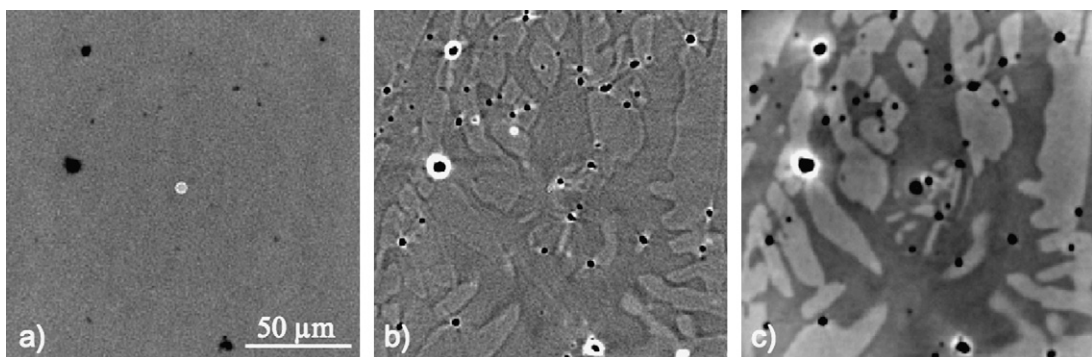


Fig. 3. Comparison of (a) absorption contrast, (b) phase sensitive and (c) holotomographic reconstruction of the two-phase microstructure in an austenitic/ferritic duplex steel. Black dots correspond to porosities in the as cast microstructure.

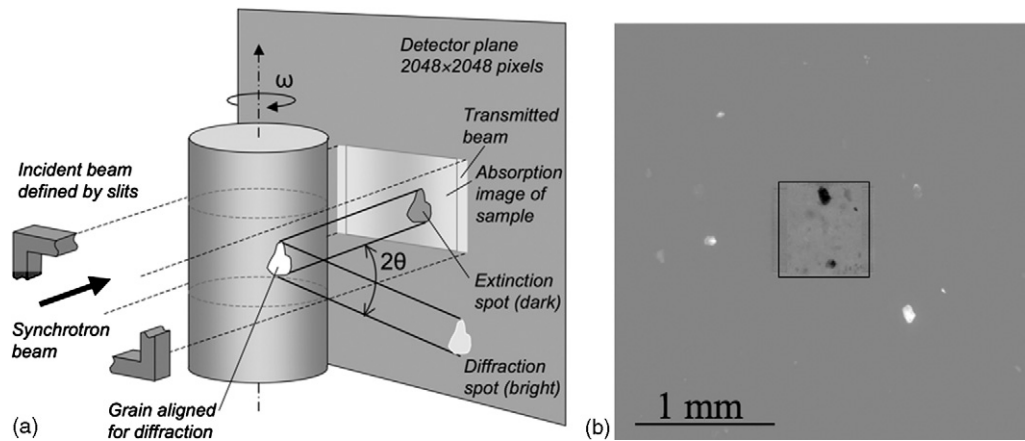


Fig. 4. (a) Experimental setup for DCT, allowing for simultaneous acquisition of absorption and diffraction information by proximity of sample and detector. (b) Example of preprocessed image—remaining contrasts are due to Bragg diffraction of individual grains.

Step 1: The diffraction spots are segmented using thresholding techniques and information about the spots is stored in a database (position, intensity, area, etc.).

Step 2: From axial symmetry consideration a grain which diffracts for an angular position ω diffracts at $\omega + 180^\circ$. These pairs of diffraction spots are detected automatically using a combination of spatial and crystallographic criteria. Once a pair of spots is detected, the diffraction angles describing the geometry of the diffraction event (plane normal, scattering vector) can be calculated. Step 3: The next step consists in sorting diffraction spots into sets belonging to the same grain (“indexing”). This is done by checking both spatial and crystallographic consistency criteria. The diffracted beams arising from a grain have to intersect at the grain position, and the angle between scattering vectors has to reflect the crystal symmetry. The set of scattering vectors is used to compute the crystallographic orientation of the grain. For this calculation the Rodrigues space representation of orientation space is used. The resultant Rodrigues vector represents the rotation required to bring the crystal axes into coincidence with the global reference frame.

Step 4: In the absence of strong orientation and strain gradients within a grain, the diffraction spots can be considered as projections of the grain from which they arise. They are used to reconstruct the three-dimensional grain shape using algebraic reconstruction techniques (ART) [38]. This algorithm allows the reconstruction of 3D structure from a limited number of projections. Each grain is reconstructed individually. The assembly of all the reconstructed grains produces the 3D grain microstructure of the sample (Fig. 5).

Step 5: The direct beam images recorded during the scan are used to reconstruct the absorption contrast tomogram of the sample by conventional filtered backprojection reconstruction [4]. The 3D tomogram obtained is superimposed on the 3D grain map determined by DCT.

4. In situ observation of recrystallization process in Al by toptomography

Dynamic studies related to recrystallization and grain coarsening processes in the bulk of monophase materials require good temporal and spatial resolution in order to capture details of the 3D shape evolution within reasonable experiment time.

One possible way of improving the spatial and temporal resolution of diffraction contrast tomography consists in switching to a modified acquisition geometry, termed toptomography [27,28]. This variant of 3D diffraction imaging enables fast (minutes compared to hours for DCT) imaging of *one individual grain* with a detector resolution that can be tailored to the dimensions of the grain rather than to a multiple of the sample dimensions. From an instrumental point of view toptomography requires additional degrees of freedom, since one of the lattice plane normals of the grain has to be aligned parallel to the tomographic rotation axis. Compared to conventional tomographic alignment, the rotation axis is inclined by the Bragg angle θ_{Bragg} with respect to the incoming beam and a small rocking movement $\Delta\theta$ is performed at each rotation position in order to fully illuminate the diffracting grain. Since this alignment offers the possibility to acquire a large number of equally spaced projections it can be used in combination

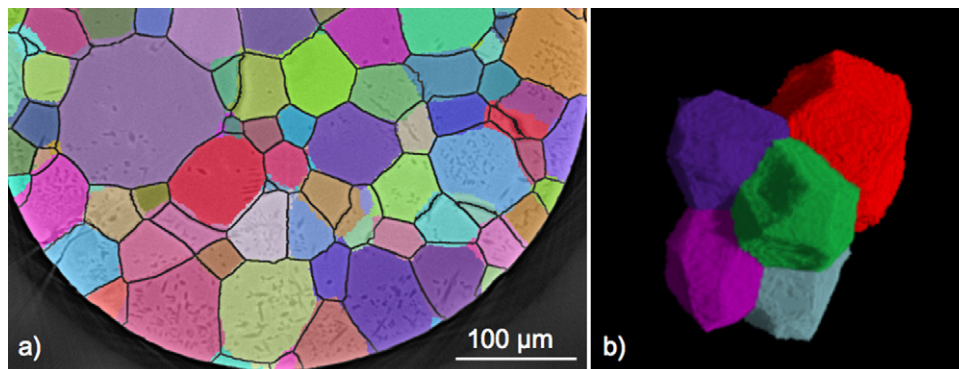


Fig. 5. (a) Overlay of grain reconstruction in Ti alloy (TIMET β 21S) produced by DCT (coloured outlines) with the real microstructure as determined from phase contrast tomography (black lines) (b) 3D rendition of a small grain cluster (DCT data). (For interpretation of the references to color in this figure legend, the reader is referred to the web version of the article.)

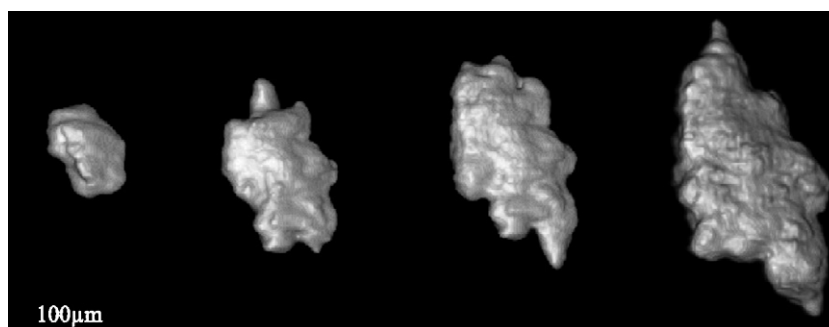


Fig. 6. Snapshots of a growing grain, imaged by topotomography. The growth into the deformed microstructure of the matrix material shows some pronounced, finger-like protrusions.

with well established arithmetic reconstruction algorithms (filtered backprojection).

Whereas previous studies aimed at optimum spatial resolution in order to resolve structures inside the grain [28], we present here an example optimized for time resolution. In cases where the principal goal is to obtain information about the 3D grain outline, one may reduce the number of projections and use algebraic reconstruction algorithms [38] capable of producing good shape reconstruction with a limited number of projections. The described fast acquisition procedure was used for studying the dynamics of the recrystallization process in Al alloy 1050. Some preliminary results are illustrated in Fig. 6 showing four out of a series of 40 time steps acquired during the evolution of an initially small grain, growing into the deformed (non-recrystallized) microstructure of the base material. Each time step consisted in the acquisition, at room temperature, of a tomographic scan comprising 45 projection over 360°, followed by a 20 s annealing cycle. At the spatial resolution employed in this study (2.8 μm pixel size), the total acquisition time for one scan was 10 min. The annealing was performed on the tomographic setup by translating the sample in and out of a stream of hot air, produced by a furnace that was set to a temperature of 160 °C.

5. Combined use of DCT and μCT applied to the study of brittle fracture

One of the particular strength of DCT is its compatibility with state of the art synchrotron radiation microtomography acquisition procedures. For instance, given a beam offering sufficient degree of spatial coherence, DCT and phase contrast tomography can be performed on the same instrument—with no or minor changes to the experiment conditions (for optimum spatial and temporal resolution in phase contrast imaging switching to a large bandwidth multilayer monochromator and adjustment of the detector resolution to the sample dimensions may be required).

An example illustrating the potential of such combined diffraction experiments is shown in Fig. 7. In this case the failure of a polycrystalline alumina material by intergranular brittle fracture was studied. To minimise disturbances to the sample and possible misalignments between acquisitions, the same sample environment and detector optics were used for both DCT and SRμCT. The only changes in configuration were in the sample-detector distance, which was increased for tomography to provide some phase contrast edge enhancement, and the position of the rotation axis, which was shifted away from the centre of the synchrotron beam to increase the region imaged (half acquisition concept, see for example [39]). The grain structure of the material was first imaged using DCT as described in section three. The sample was then loaded in compression in situ, and a series of tomograms recorded with increasing load until failure occurred. The absorption contrast

tomograms show the intergranular pores (Fig. 7a) that are present in the as-received material (mainly located at grain boundaries and boundary triple junctions) and the intergranular cracking that developed during the final loading increment (Fig. 7b). The overlay of the absorption image after cracking with the DCT grain map, shown in Fig. 7c, reveals the intergranular character of the damage which developed from the combined action of compression and residual strains arising from anisotropy of the thermal expansion and elastic coefficients. The information from the DCT map will allow grain boundaries characteristics to be analysed, for example by comparison with predicted intergranular thermal strains to elucidate the relative importance of grain orientations and grain boundary structures.

6. Discussion

6.1. Spatial resolution and applicability of different approaches

Among the techniques presented in this paper, the microtomographic imaging methods described in Section 2 offer the highest spatial resolution and accuracy. The ultimate resolution in parallel beam X-ray imaging is determined by the X-ray to visible light conversion process in the luminescent screen and the modulation transfer function of the light optical system coupling the screen to the charge coupled device camera. Values down to about 0.5 μm FWHM have been measured for the point spread function of state of the art high-resolution X-ray imaging detectors [40]. However, a problem frequently encountered in grain boundary decoration techniques is the dependency of the wetting/precipitation behaviour on the grain boundary energy. Low energy boundary configurations may result in incomplete decoration of the boundary network, leading to problems in automated grain segmentation procedures. On the other hand, selective wetting behaviour opens interesting possibilities for combined microtomography and DCT characterization in these material systems, since the local wetting/precipitation behaviour can be correlated with a 5-parameter description of the grain boundary character (misorientation and crystallographic habit plane) on a statistically relevant number of grain boundaries [41].

In DCT only a fraction of the detector dimensions are used for acquisition of the absorption information. Therefore the spatial resolutions of both the grain map and the simultaneously obtained absorption contrast tomogram are about 3–4 times worse compared to the ultimate spatial resolution achievable in (parallel beam) absorption and/or phase contrast microtomography. The oblique incidence of diffracted beams on the detector and the distortion of the diffraction spots arising from local variations of the scattering vector are additional factors affecting the ultimate spatial resolution and accuracy achievable with the current DCT analysis procedure. The algebraic reconstruction process is based on the assumption that individual diffraction spots can be treated as par-

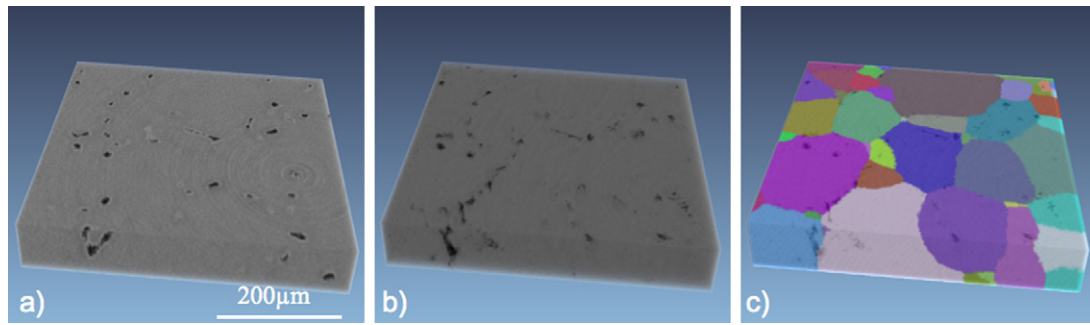


Fig. 7. (a) 3D rendition of a subvolume before cracking, (b) identical subvolume at higher applied load, showing the presence of intergranular cracks (reduced quality due to damage development during scan acquisition) (c) superimposition of DCT grain map with the absorption volume acquired in the cracked state (b), revealing the intergranular character of the cracks.

allel projections of the diffracting grain volume. This assumption is violated when significant elastic strain and/or orientation gradients build up inside a grain. For this reason, the technique can in its present state not compete with established electron microscopy (EBSD) or polychromatic X-ray scanning microprobe techniques [19,20], neither in terms of spatial resolution nor in terms of applicability to deformed microstructures. Although moderate strains and orientation gradients (up to $\sim 1^\circ$ per grain) do not prevent the production of a DCT grain map, they do affect its ultimate accuracy.

On the other hand, none of the above mentioned raster scanning techniques provide *simultaneous, non-destructive 3D* characterization of *bulk* polycrystalline samples (up to several mm in size for large grained, low Z materials [42]), containing more than one thousand grains in terms of local attenuation, grain shape and crystallographic orientation. This unique combination provides new insight into microstructure sensitive damage and deformation mechanisms like stress corrosion cracking [43] and short fatigue crack propagation (work in progress), to mention only two of them.

One experimental challenge encountered for time-lapse observations of grain deformation and coarsening processes, requiring successive DCT characterization is the accommodation of sample environment (furnace, mechanical test rigs, etc.). This problem is alleviated by the fact that some applications require only knowledge of the initial microstructure and the subsequent observation of the dynamic process (crack propagation, corrosion) can be performed by SR μ CT at larger propagation distances allowing the accommodation of sample environment [43]. For the case of multi-crystalline samples (few tens of grains) earlier variants of DCT [15] exploiting the extinction contrast in the direct beam can be considered as an alternative solution.

6.2. Perspectives

Efforts are under way to estimate the average elastic strain state for each individual grain from accurate measurement of a set of diffraction vectors—either directly from the near field DCT data [44] or, alternatively, from data acquired on a low resolution 2D diffrac-

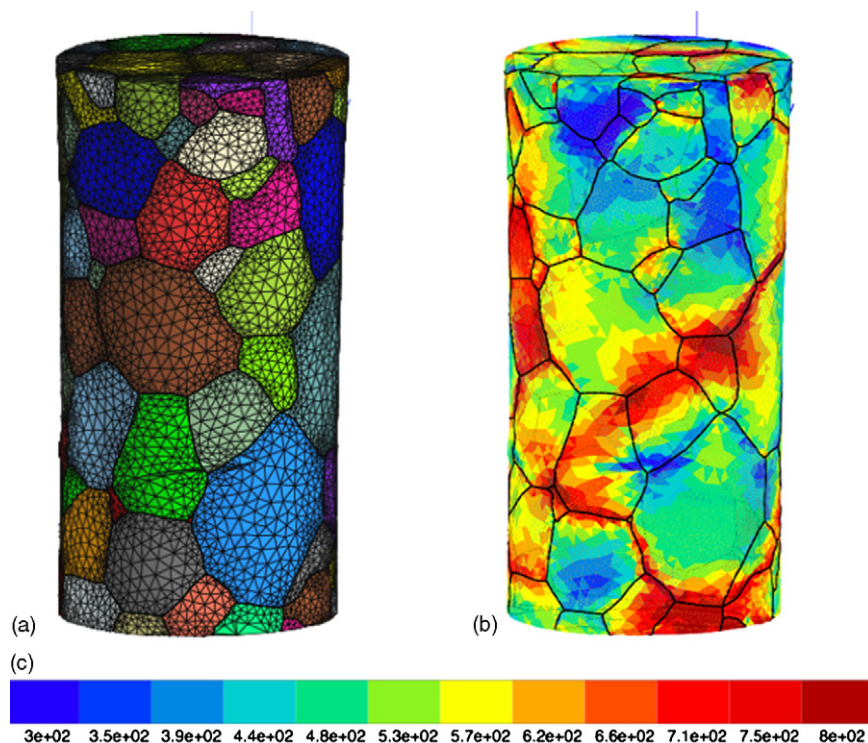


Fig. 8. (a) Finite element mesh representation of grain microstructure in a large grained beta Titanium alloy sample, as determined by DCT. (b) Predicted distribution of von Mises stress when loading the sample to 500 MPa. (c) Colour code of FEM simulation (b); units: MPa. (For interpretation of the references to color in this figure legend, the reader is referred to the web version of the article.)

tion detector positioned at intermediate distances [45]. Access to such data would give a first possibility for direct comparison of in situ deformation experiments with crystal plasticity finite element simulations (CPFEM).

As illustrated by the elastic FEM simulation based on a real grain microstructure obtained by DCT (Fig. 8a), the elastic anisotropy of grains leads to spatially varying distribution of strain and stress inside the grains, with local concentration at the grain boundaries (Fig. 8b). Such local stress concentrations play an important role in damage initiation and improved characterization capabilities for local stress and strain fields inside the bulk of materials would allow us to improve our understanding of material failure mechanisms and provide guidance for the design of materials offering increased damage resistance.

This motivates the development of improved data acquisition and analysis procedures capable of mapping local elastic strain and sub-grain misorientation distributions during the onset of plastic deformation.

For investigation of the deformation behaviour at strain values beyond the current applicability range of DCT one may consider the mapping of an undeformed microstructure containing a fine dispersion of internal markers (such as porosities, precipitates or inclusions) by means of DCT and subsequent characterization of the deformation gradient tensor field at larger strains by means of 3D digital image correlation on 3D volumes obtained by SR μ CT [46,47].

7. Conclusions

Different possibilities for non-destructive characterization of 3D grain microstructures in polycrystalline materials using synchrotron radiation X-ray imaging and diffraction techniques have been presented. Methods based on absorption and/or phase contrast imaging are limited to a few specific material systems where a second phase at the grain boundary can be detected via differences in attenuation and/or electron density. A less material specific and more complete description of the microstructure in terms of crystallographic orientation and 3D grain shape can be obtained by X-ray diffraction contrast tomography, combining the principles of three-dimensional X-ray diffraction microscopy (3DXRD), X-ray diffraction imaging (topography) and image reconstruction from projections (computed tomography). DCT applies to large grained mono (or dual-) phase materials displaying limited levels of plastic deformation and/or orientation gradients within individual grains. Sharing a common experimental setup, DCT is easily combined with state of the art 3D synchrotron imaging techniques (e.g. holotomography) and thereby offers quantitative, comprehensive description of the material's microstructure at the micrometre lengthscale, in terms of 3D grain shape, orientation, local attenuation and/or electron density distribution. The 3D grain maps produced can be used as input for simulation techniques taking the local anisotropic behaviour of the material explicitly into account. The non-destructive character and possible combination with in situ tomographic observations enables quantitative comparison of model predictions with the experimentally observed material behaviour.

Acknowledgements

We thank Richard Fonda for providing samples and sharing his experience in heat treatment. We further acknowledge the staff from beamlines ID19 and ID11 at ESRF for their assistance during experiments as well as Jose Baruchel and Sybrand van der Zwaag for their support of the work. W.L., E.M.L., S.S. and H.F.P. acknowledge the Danish National Research Foundation for sup-

porting the Center for Fundamental Research: Metal Structures in 4D, within which part of this work was performed and E.M.L. furthermore acknowledges the support jointly sponsored by the Office of Naval Research and DARPA as part of the Dynamic 3-D Digital Structure Program (Grant number N00015-05-1-0510). A.K. acknowledges funding received from the Engineering and Physical Sciences Research Council and S.R. acknowledges funding received in the framework of the French ANR project ANR-06-BLAN 0396-01.

References

- [1] J. Baruchel, J.Y. Buffiere, P. Cloetens, M. Di Michiel, E. Ferrie, W. Ludwig, E. Maire, L. Salvo, *Scripta Mater.* 55 (2006) 41–46.
- [2] J. Baruchel, P. Bleuet, A. Bravin, P. Coan, E. Lima, A. Madsen, W. Ludwig, P. Pernot, J. Susini, *C. R. Phys.* 9 (5–6) (2008) 624–641.
- [3] S.R. Stock, *Microcomputed Tomography: Methodology and Applications*, CRC Press, 2009.
- [4] A.C. Kak, M. Slaney, *Principles of Computerized Imaging*, IEEE Press, 1988.
- [5] A. Snigirev, I. Snigireva, V. Kohn, S. Kuznetsov, I. Schelokov, *Rev. Sci. Instrum.* 66 (1995) 5486.
- [6] P. Cloetens, R. Barrett, J. Baruchel, J.P. Guigay, M. Schlenker, *J. Phys. D: Appl. Phys.* 29 (1996) 133.
- [7] P. Cloetens, M. Pateyron-Salomé, J.Y. Buffière, G. Peix, J. Baruchel, F. Peyrin, M. Schlenker, *J. Appl. Phys.* 81 (1997) 5878.
- [8] U. Bonse, M. Hart, *Appl. Phys. Lett.* 6 (1965) 155.
- [9] T. Weitkamp, A. Diaz, C. David, F. Pfeiffer, M. Stampanoni, P. Cloetens, E. Ziegler, *Opt. Expr.* 13 (2005) 6296–6304.
- [10] D. Chapman, W. Thomlinson, R.E. Johnston, D. Washburn, E. Pisano, N. Gmür, Z. Zhong, E. Menk, F. Arfelli, D. Sayers, *Phys. Med. Biol.* 42 (1997) 2015.
- [11] P. Cloetens, W. Ludwig, J. Baruchel, D. Van Dyck, J. Van Landuyt, J.P. Guigay, M. Schlenker, *Appl. Phys. Lett.* 75 (1999) 2912–2914.
- [12] S.R. Stock, A.E.M. Vieira, A.C.B. Delbem, M.L. Cannon, X. Xiao, F.J. De Carlo, *J. Struct. Biol.* (2008) 161–162.
- [13] P. Bleuet, E. Welcomme, E. Dooryhée, J. Susini, J.L. Hodeau, P. Walter, *Nat. Mater.* 7 (2008) 468–472.
- [14] B.K. Tanner, *X-ray Diffraction Topography*, Pergamon Press, Oxford, 1976.
- [15] W. Ludwig, S. Schmidt, E.M. Lauridsen, H.F. Poulsen, *J. Appl. Cryst.* 41 (2008) 302–309.
- [16] G. Johnson, A. King, M. Gonclaves Honnicke, J. Marrow, W. Ludwig, *J. Appl. Cryst.* 41 (2008) 310–318.
- [17] W. Ludwig, P. Reischig, A. King, M. Herbig, E.M. Lauridsen, T.J. Marrow, J.Y. Buffiere, *Rev. Sci. Instrum.* 80 (2009) 033905.
- [18] H.F. Poulsen, *Three-Dimensional X-ray Diffraction Microscopy. Mapping Polycrystals and their Dynamics*. Springer Tracts in Modern Physics, Springer, Berlin, 2004.
- [19] B.C. Larson, W. Yang, G.E. Ice, J.D. Budai, J.Z. Tischler, *Nature* 415 (2002) 887–890.
- [20] G.E. Ice, B.C. Larsen, W. Yang, J.D. Budai, J.W.L. Pang, R.I. Barabash, W. Lui, *J. Synchrotron Radiat.* 12 (2005) 155–162.
- [21] H.F. Poulsen, S.F. Nielsen, E.M. Lauridsen, S. Schmidt, R.M. Suter, U. Lienert, L. Margulies, T. Lorentzen, D. Juul Jensen, *J. Appl. Cryst.* 34 (2001) 751–756.
- [22] S. Nielsen, W. Ludwig, D. Bellet, E. Lauridsen, H. Poulsen, D.J. Jensen, *Proc. 21st Risoe Int. Symposium on Materials Science*, vol. 21, 2001, pp. 473–478.
- [23] X. Fu, H.F. Poulsen, S. Schmidt, S.F. Nielsen, E.M. Lauridsen, D. Juul Jensen, *Scripta Mater.* 49 (2003) 1093.
- [24] T. Markussen, X. Fu, L. Margulies, E.M. Lauridsen, S.F. Nielsen, S. Schmidt, H.F. Poulsen, *J. Appl. Cryst.* 37 (1) (2004) 96–102.
- [25] R.M. Suter, D. Hennessy, C. Xiao, U. Lienert, *Rev. Sci. Instrum.* 77 (2006) 123905.
- [26] S. Schmidt, U.L. Olsen, H.F. Poulsen, H.O. Sørensen, E.M. Lauridsen, L. Margulies, C. Maurice, D. Juul Jensen, *Scripta Mater.* 59 (2008) 491–494.
- [27] W. Ludwig, P. Cloetens, J. Härtwig, J. Baruchel, B. Hamelin, P. Bastie, *J. Appl. Cryst.* 34 (2001) 602–607.
- [28] W. Ludwig, E.M. Lauridsen, S. Schmidt, H.F. Poulsen, J. Baruchel, *J. Appl. Cryst.* 40 (2007) 905–911.
- [29] M.G. Nicholas, *C.F. Old, J. Mater. Sci.* 14 (1979) 1.
- [30] W. Ludwig, D. Bellet, *Mater. Sci. Eng. A* 281 (2000) 198–203.
- [31] E. Pereiro-Lopez, W. Ludwig, D. Bellet, P. Cloetens, C. Lemaignan, *Phys. Rev. Lett.* 95 (21) (2005) 215501.
- [32] W. Ludwig, J.Y. Buffiere, S. Savelli, P. Cloetens, *Acta Mater.* 51 (2003) 585–598.
- [33] E. Ferrie, J.-Y. Buffiere, W. Ludwig, *Int. J. Fatigue* 27 (2005) 1215–1220.
- [34] T. Ohgaki, H. Toda, I. Sinclair, J.-Y. Buffiere, W. Ludwig, T. Kobayashi, M. Niinomi, T. Akahori, *Mater. Sci. Eng. A* 427 (2006) 1–6.
- [35] H. Proudhon, J.-Y. Buffiere, S. Fouvry, *Eng. Fract. Mech.* 74 (2007) 782–793.
- [36] K.H. Khor, J.-Y. Buffiere, W. Ludwig, I. Sinclair, *Scripta Mater.* 55 (2006) 47–50.
- [37] S.R. Dey, E.M. Lauridsen, W. Ludwig, D.J. Rowenhorst, R.W. Fonda, in: M. Niinomi, S. Akiyama, M. Ikeda, M. Hagiwara, K. Maruyama (Eds.), *Proceedings of Ti-2007 Science and Technology*, The Japan Institute of Metals, 2007, pp. 467–470.
- [38] R. Gordon, R. Bender, G.T. Herman, *J. Theor. Biol.* 29 (1970) 471–481.
- [39] A. Mazurier, V. Volpato, R. Macchiarelli, *Appl. Phys. A* 83 (2006) 229–233.
- [40] T. Martin, A. Koch, *J. Synchrotron Radiat.* 13 (2006) 180.
- [41] P. Wynblatt, M. Takashima, *Interface Sci.* 9 (2001) 265–273.

- [42] S. Rolland du Roscoat, A. King, A. Philip, P. Reischig, W. Ludwig, F. Flin, J. Meyssonnier, submitted for publication.
- [43] A. King, G. Johnson, D. Engelberg, W. Ludwig, J. Marrow, *Science* 321 (2008) 382–385.
- [44] P. Reischig, Determination of elastic strain tensors of individual grains in polycrystals by means of diffraction contrast tomography, Master of science Thesis, Delft University of Technology, 2008.
- [45] R.V. Martins, L. Margulies, S. Schmidt, H.F. Poulsen, T. Leffers, *Mater. Sci. Eng. A* 387–389 (2004) 84.
- [46] S.F. Nielsen, H.F. Poulsen, F. Beckmann, C. Thorning, J.A. Wert, *Acta Mater.* 51 (2003) 2407.
- [47] J. Rethore, J.-P. Tinnes, S. Roux, J.-Y. Buffiere, F. Hild, *Comptes rendus de Mecanique* 336 (2008) 643–649.